the FEBS Journal

Rational design of a conformation-switchable Ca^{2+}- and Tb^{3+}-binding protein without the use of multiple coupled metal-binding sites

Shunyi Li[1,2], Wei Yang[3], Anna W. Maniccia[1], Doyle Barrow Jr[1], Harianto Tjong[4], Huan-Xiang Zhou[4] and Jenny J. Yang[1]

1 Department of Chemistry, Center of Drug Design and Biotechnology, Georgia State University, Atlanta, GA, USA
2 College of Life Sciences, Hubei University, Wuhan, China
3 Changchun Institute of Applied Chemistry, Chinese Academy of Sciences, Changchun, Jilin, China
4 Department of Physics and Institute of Molecular Biophysics and School of Computational Science, Florida State University, Tallahassee, FL, USA

Keywords
Ca^{2+} binding; conformational change; protein design; Tb^{3+} binding; trigger

Correspondence
J. J. Yang, 50 Decatur Street, Atlanta, GA 30303, USA
Fax: +1 404 413 5551
Tel: +1 404 413 5520
E-mail: chejjy@langate.gsu.edu

(Received 14 May 2008, revised 10 July 2008, accepted 12 August 2008)

doi:10.1111/j.1742-4658.2008.06638.x

Ca^{2+}, as a messenger of signal transduction, regulates numerous target molecules via Ca^{2+}-induced conformational changes. Investigation into the determinants for Ca^{2+}-induced conformational change is often impeded by cooperativity between multiple metal-binding sites or protein oligomerization in naturally occurring proteins. To dissect the relative contributions of key determinants for Ca^{2+}-dependent conformational changes, we report the design of a single-site Ca^{2+}-binding protein (CD2.trigger) created by altering charged residues at an electrostatically sensitive location on the surface of the host protein rat Cluster of Differentiation 2 (CD2). CD2.trigger binds to Tb^{3+} and Ca^{2+} with dissociation constants of 0.3 ± 0.1 and 90 ± 25 μM, respectively. This protein is largely unfolded in the absence of metal ions at physiological pH, but Tb^{3+} or Ca^{2+} binding results in folding of the native-like conformation. Neutralization of the charged coordination residues, either by mutation or protonation, similarly induces folding of the protein. The control of a major conformational change by a single Ca^{2+} ion, achieved on a protein designed without reliance on sequence similarity to known Ca^{2+}-dependent proteins and coupled metal-binding sites, represents an important step in the design of trigger proteins.

Ca^{2+}-dependent conformational change is a common mechanism for signal transduction, which regulates the interactions of trigger proteins with downstream partners and target molecules [1–6]. Trigger proteins can respond to Ca^{2+} concentration changes in different cellular environments through cooperative binding/dissociation of multiple Ca^{2+} ions [3]. For example, on binding four Ca^{2+} ions, calmodulin (CaM) exhibits a large rearrangement of the flexible Ca^{2+}-binding loops and the helical packing of paired EF-hand motifs, which affords CaM the ability to regulate more than 100 target proteins in various biological processes [4–6]. Conversely, troponin C, with a strong sequence and structural similarity to CaM, specifically interacts with troponin I to control muscle contraction. Extracellularly, Ca^{2+}-sensing receptors and other sensing proteins each bind to several Ca^{2+} ions cooperatively to activate multiple signaling pathways in the cytosol through conformational changes.

Abbreviations
ANS, 8-anilinonaphthalene-1-sulfonate; CaM, calmodulin; CD2, cluster of Differentiation 2; FRET, fluorescence resonance energy transfer; ITC, isothermal titration calorimetry; PB, Poisson–Boltzmann.

Electrostatic interactions have been proposed to be important for Ca^{2+}-induced conformational change, as well as for Ca^{2+}-binding affinity and protein stability [7–9]. Statistical analyses have shown that Ca^{2+} ions are predominantly coordinated to oxygen from carboxylate, carbonyl and hydroxyl groups in proteins [10–12]. A Ca^{2+}-binding site in proteins has an average coordination number of six to seven, arranged in either a pentagonal bipyramidal or distorted octahedral geometry. Proteins that exhibit large Ca^{2+}-induced conformational changes usually have a large number of charged residues in the Ca^{2+}-binding sites. Although the clustering of negatively charged residues favors the attraction of positively charged Ca^{2+} ions, it may also force a conformational rearrangement of the coordination residues, or even the entire protein, in the absence of Ca^{2+}. In addition, structural studies have revealed large ensembles of conformations of trigger proteins in different states. However, the determinants for Ca^{2+} binding and Ca^{2+}-dependent conformational changes have yet to be clearly elucidated. To date, the development of novel Ca^{2+}-dependent proteins has been based on the mimicking of the natural Ca^{2+}-binding proteins with multiple coupled metal-binding sites [13]. Chazin and colleagues [14] reported elegant work on the creation of the CaM-like Ca^{2+}-dependent conformational change in calbindin D_{9k} by replacing residues in calbindin D_{9k} with the corresponding residues of CaM. However, it is unclear whether it is possible to achieve calcium-dependent conformational change without the use of coupled metal-binding sites.

A major barrier to understanding the molecular mechanism of Ca^{2+}-dependent biological functions is the lack of established rules relating Ca^{2+}-binding affinity to specific structural aspects of proteins [15,16]. This is exacerbated by the complexities encountered in cooperative, multi-site systems, and the use of Ca^{2+}-binding energy to effect conformational changes in proteins such as CaM [17]. Obtaining information for calcium-induced conformational change is limited by the measurement of Ca^{2+}-binding affinities for site-specific Ca^{2+} binding and cooperativity [15].

To overcome the limitations associated with naturally occurring Ca^{2+}-binding proteins, our laboratory has developed an approach to dissect the key structural factors that control Ca^{2+}-binding affinity, Ca^{2+}-dependent conformational changes and cooperativity by designing a single Ca^{2+}-binding site in a model protein [13,14]. Departing from previously published studies that have mimicked natural Ca^{2+}-binding proteins [18–20], we have demonstrated the successful design of an array of single Ca^{2+}-binding sites using the host protein rat Cluster of Differentiation 2 (CD2). For example, the single Ca^{2+}-binding site in Ca.CD2 has been shown to be capable of resisting global conformational changes on Ca^{2+} binding, and solution structures have demonstrated that Ca^{2+} binds at the intended site with the designed arrangements [19,21,22]. This model system has been used to dissect local factors important for calcium-binding affinity [20,21,23].

In this paper, we report the successful design of a trigger protein (CD2.trigger) that can be used as a model system to reveal key factors essential for Ca^{2+}-dependent conformational changes. CD2 has a common Ig fold with nine β-strands sandwiched in two layers (Fig. 1A) [24,25], similar to that of the Ca^{2+}-dependent molecules cadherin and C2 domains [26]. Results from a designed Ca^{2+}-binding CD2 can directly aid in the study of these proteins. In addition, CD2 can be reversibly refolded [27], which is important for the study of Ca^{2+}-dependent conformational change and Ca^{2+}-dependent biological function. Unlike our previously designed Ca^{2+}-binding proteins, the design of CD2.trigger is created by altering charged residues at an electrostatically sensitive location, based on the hypothesis that Ca^{2+}-dependent protein folding can be achieved by Ca^{2+} binding to reduce the electrostatic repulsion in the apo protein. Two positively charged residues, Arg31 and Lys43, that form a network of salt bridges with Glu29 and Glu41 were mutated to acidic residues to form a Ca^{2+}-binding pocket. In contrast with conformational changes elicited by cooperative binding of multiple Ca^{2+} ions to natural proteins, the designed CD2.trigger exhibits a major conformational change on binding of a single Ca^{2+} ion, revealed by various spectroscopic methods.

Results

Design of a Ca^{2+}-modulating protein

The design of a Ca^{2+}-binding protein with a Ca^{2+}-induced global conformational change was based on several considerations. First, as natural Ca^{2+} trigger proteins often have Ca^{2+}-induced folding instead of Ca^{2+}-induced unfolding, we assumed that the Ca^{2+}-bound protein would possess the wild-type CD2 structure. Therefore, we performed computational design of the Ca^{2+}-binding site based on the local geometric properties of a target site in the host protein by assuming that the backbone of the protein was not altered [18–20]. Second, to ensure the strong Ca^{2+}-binding energy required for protein folding, it was determined

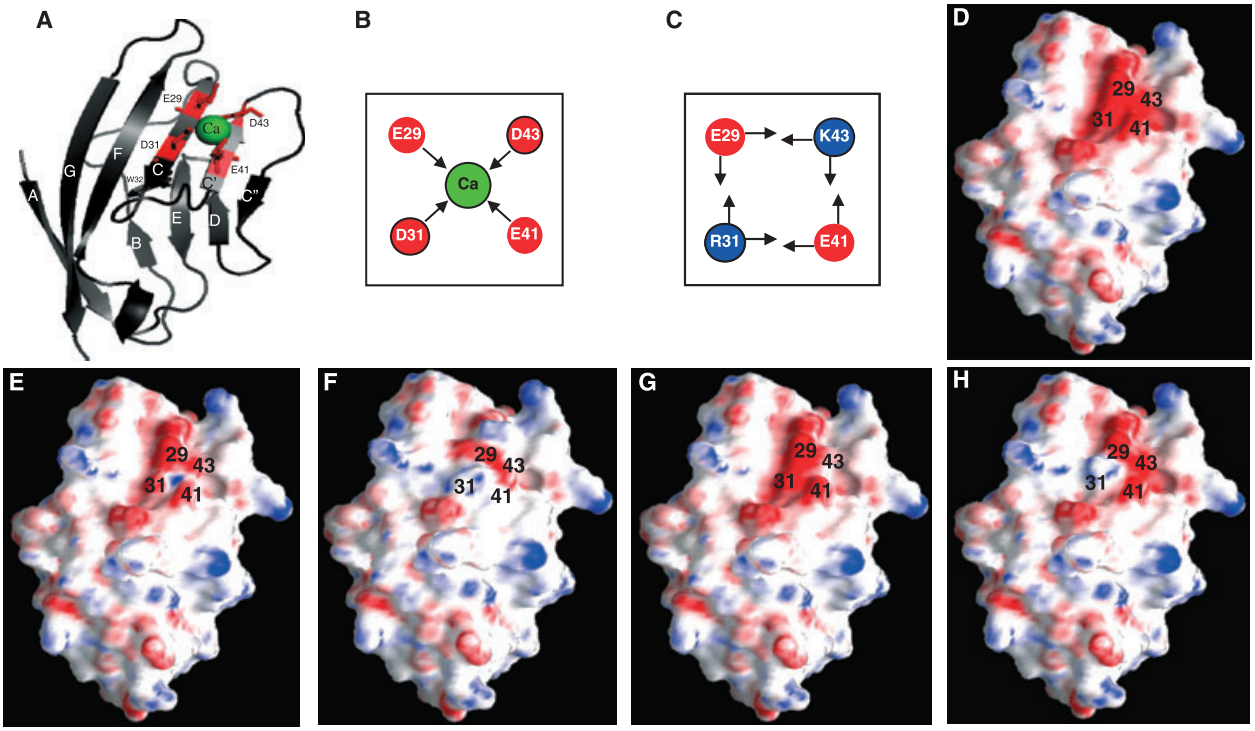

Fig. 1. Protein design and calculation. (A) Model structure of designed Ca^{2+}-binding protein CD2.trigger with Ca^{2+} coordination residues Glu29, Asp31, Glu41 and Asp43 based on CD2 (1hng). This structure was drawn using the program PYMOL (DeLano Scientific LLC, Palo Alto, CA, USA). (B,C) Local electrostatic interactions in CD2.trigger (B) and wild-type CD2 (C). (D–H) Surface electrostatic potentials of metal-free CD2.trigger, Ca^{2+}-loaded CD2.trigger, wild-type CD2, metal-free R31D/K43N and metal-free R31K/K43D, respectively.

that a minimum of four negatively charged coordination residues should be utilized, based on results observed from our previous designs of Ca^{2+}-binding proteins, which indicated no global conformational changes following the introduction of two to three negatively charged coordination residues [20,21,23]. Third, regions on the protein surface with high electrostatic potential (electrostatic 'hotspots') are typically sensitive to changes in electrostatic interactions on binding of metal ions. Therefore, we hypothesized that, if repulsion of the cation coordination residues leads to the unfolding of the apo protein, neutralization of these charges by Ca^{2+} binding may trigger the refolding of the protein.

Figure 1A shows the model structure of the designed protein, denoted as CD2.trigger, with a Ca^{2+}-binding site introduced into an electrostatic 'hotspot' on CD2. The coordination shell of the site contains four negatively charged residues located at the center of the densely charged GFCC′C″ surface of the CD2 sandwich layers. The site was formed by two reverse charge mutations, R31D and K43D, together with the existing residues Glu29 and Glu41 (Fig. 1A,B). The mutations disrupt the charge balance at the site and the surrounding salt bridge networks. In wild-type CD2, Arg31, Lys43, Glu29 and Glu41 form several salt bridges (Fig. 1C). In addition, they are involved in salt bridges with surrounding charged residues. A strong negative surface electrostatic potential is produced by the purported Ca^{2+} coordination residues and the surrounding negative residues, such as Asp28 and Glu33, as calculated by the DELPHI program [28].

Metal-binding affinity and selectivity

Fig. S1 shows the ESI mass spectra of CD2.trigger variants. The addition of excess Ca^{2+} or La^{3+} resulted in the appearance of a new mass peak corresponding to CD2.trigger–metal complex with a stoichiometry of 1 : 1. By monitoring the NMR chemical shift changes as a function of Ca^{2+} concentration, a K_d value of 90 ± 25 μM was obtained. This is comparable with the K_d value of 240 ± 20 μM obtained from isothermal titration calorimetry (ITC) (Fig. 2B). The ITC study further revealed that Ca^{2+} binding of CD2.trigger was a slightly exothermic process. The small magnitude of heat released was very similar to the compensation of enthalpy change by the endothermic Ca^{2+}-induced

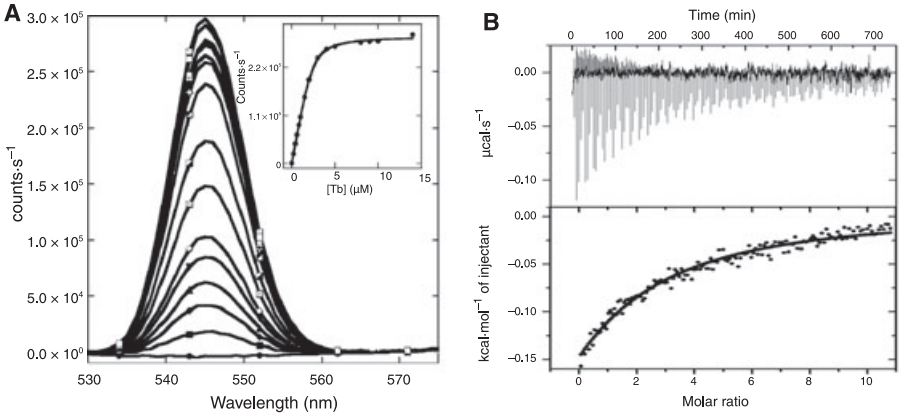

Fig. 2. Metal-binding affinities. (A) Fluorescence emission spectra of CD2.trigger (excited at 280 nm) in 10 mM Pipes/10 mM KCl, pH 6.8, with 0, 0.2, 0.4, 0.6, 0.8, 1.0, 1.5, 2.0, 3.0, 4.0, 5.0, 6.0, 7.0, 8.0, 9.0, 10 or 14 μM Tb^{3+} (bottom to top). The fluorescence enhancement at 545 nm as a function of Tb^{3+} concentration was fitted assuming the formation of a 1 : 1 protein–Tb^{3+} complex (inset). (B) Ca^{2+} titration of CD2.trigger by ITC at 5 °C. A solution of 5 mM $CaCl_2$ was titrated in increments of 2 μL into 0.1 mM protein.

conformational change observed for the trigger protein CaM [29], as well as the Zn^{2+}-induced folding of zinc fingers [30]. However, it was very different from the binding process observed on the nontrigger protein α-lactalbumin. Unfortunately, the small change in the isotherm prevented us from obtaining the stoichiometry. The calculated ΔH and ΔS values for Ca^{2+} binding to CD2.trigger were -0.93 ± 0.02 kcal·mol^{-1} and 11.6 ± 0.02 cal·mol^{-1}·K^{-1}, respectively. This ΔH value is several-fold smaller in magnitude than that of Ca^{2+} binding to α-lactalbumin, with reported values of -1.7 kcal·mol^{-1} at 5 °C and -59 kcal·mol^{-1} at 45 °C in Tris/HCl buffer at pH 8.0 [31]. The formation of precipitation limits further the ITC study of Tb^{3+} binding to CD2.trigger variants.

Tb^{3+} binding to CD2.trigger produced a large fluorescence enhancement at 545 nm as a result of fluorescence resonance energy transfer (FRET) on excitation at 280 nm (Fig. 2A). The R31K/K43D variant showed a significant decrease in Tb^{3+}-binding affinity, with an apparent K_d value of 5.7 ± 0.6 μM obtained using FRET, whereas the R31D/K43N variant had a K_d value of 0.22 ± 0.04 μM, similar to CD2.trigger (Fig. S4). These binding affinities were considered to be lower limits as a result of limitations in the direct titration method, such as the concentration increment and accuracy, signal-to-noise ratio and other factors. Our methods cannot measure accurately any apparent K_d values smaller than 1 μM. A decrease in metal-binding affinity by the R31K/K43D mutation was expected, as the mutations reduced the net negative charge at the metal-binding site. Such an affinity decrease was predicted by our electrostatic calculations on Ca^{2+} binding. The metal-binding affinities, using different methods, are summarized in Table 1.

It is interesting to note that the affinity for La^{3+} or Tb^{3+} is approximately 300–800-fold greater than for Ca^{2+}. Like many natural Ca^{2+}-binding proteins, CD2.trigger exhibits selective binding for Ca^{2+} and La^{3+} over excess physiological cations such as Mg^{2+}

Table 1. Metal-binding affinity and thermal stability of the designed proteins. N/A, not available.

	K_d (μM)		T_m (°C)[d]	
Protein	Ca^{2+}	Tb^{3+}[e]	EGTA	Ca^{2+}
CD2.trigger	90 ± 20[a] 240 ± 20[b]	0.3 ± 0.1[c]	52 ± 1	54 ± 1
CD2.trigger. R31K/K43D	N/A	5.7 ± 0.6[c]	56 ± 1	56 ± 1
CD2.trigger. K31D/K43N	N/A	0.2 ± 0.04[c]	55 ± 1	56 ± 1
Ca.CD2 [23]	1400 ± 400	8 ± 2	63 ± 2	63 ± 2
Wild-type CD2 [23]	N/A	N/A	61 ± 1	61 ± 1

[a] Measured by NMR in 10 mM Pipes/10 mM KCl, pH 6.8. [b] Measured by ITC in 10 mM Pipes/10 mM KCl, pH 6.8. [c] Measured by FRET in 10 mM Pipes/10 mM KCl, pH 6.8. [d] Measured by CD in 10 mM Mops/10 mM KCl, pH 6.8. [e] These binding affinities should be considered as the lower limits because of limitations of the direct titration method, such as the concentration increment and accuracy, signal-to-noise ratio and other factors. Our methods cannot measure accurately any apparent K_d values smaller than 1 μM.

and K^+. The addition of 2 mM Ca^{2+} or 1 mM La^{3+} following 100 mM K^+ or 10 mM Mg^{2+} led to significant changes in the NMR spectra, suggesting that the specific binding of Ca^{2+} and La^{3+} cannot be shielded by the excess concentrations of K^+ and Mg^{2+}. Consistently, the addition of excess Mg^{2+} (10 mM) or K^+ (> 100 mM) did not affect the Tb^{3+} fluorescence enhancement monitored by FRET.

Metal ion-dependent conformational change

CD2.trigger underwent the expected Ca^{2+}-induced conformational change revealed by various spectroscopic methods. In the absence of Ca^{2+}, Tb^{3+} or La^{3+} at physiological pH (pH 7.2), the far-UV CD spectrum of CD2.trigger had a minimum at 205 nm (Fig. 3A), suggesting the loss of the β-strand secondary structure [24,25]. In addition, the Trp fluorescence emission shifted to 341 nm (close to the 350 nm of free Trp) from the 327 nm of wild-type CD2 (Fig. 3C). This suggests that the buried Trp32 in wild-type CD2 becomes solvent exposed in CD2.trigger. In contrast, the Trp fluorescence spectrum of wild-type CD2 changed with the addition of Ca^{2+} (Fig. 3C, inset). Furthermore, the binding of the hydrophobic dye 8-anilinonaphthalene-1-sulfonate (ANS) to CD2.trigger showed a 40% increase in fluorescence intensity with a 13 nm blue shift in the emission maximum wavelength when the La^{3+} concentration was increased from 0 to 10 μM, suggesting that conformational changes of CD2.trigger were induced by La^{3+} binding (Fig. 3D). Conversely, there were no detectable changes in the wild-type CD2 spectrum (Fig. 3D, inset). In the one-dimensional NMR spectrum, the dispersed resonances around 10 and 0 p.p.m., typically observed in wild-type CD2, disappeared in the CD2.trigger spectrum, indicating the loss of tertiary packing (Fig. 4A,B). Furthermore, the loss of secondary and tertiary structures in CD2.trigger was clearly demonstrated by the heteronuclear single quantum correlation spectrum, in which all resonances were crowded into a narrow region (Fig. 4C).

Ca^{2+}, Tb^{3+} or La^{3+} binding all refolded CD2.trigger into a CD2-like structure. With the addition of Ca^{2+}, Tb^{3+} or La^{3+}, the spectra from far-UV CD, fluorescence emission and NMR were similar to those of wild-type CD2. The negative maximum at 216 nm in the CD spectrum indicated the formation of a β-strand structure, whereas the Trp emission at 333 nm and the NMR resonances in the 10 and 0 p.p.m. regions indicated the formation of a tightly packed tertiary structure. The metal-induced conformational change is highly cooperative, as shown by the concurrent formation of secondary and tertiary structures (Fig. 3). Ca^{2+} titrations showed that the fractional changes in CD signal, Trp emission fluorescence and NMR chemical shifts of different resonances coincided. As a result, the different spectroscopic methods gave similar estimates for the metal-binding affinity.

Removal of charge repulsion by protonation and mutations

We hypothesized that a major factor in the metal-binding-induced conformation change is the reduction in the charge repulsion present in the metal-binding site of CD2.trigger. To verify this hypothesis, two additional approaches were pursued to reduce the negative charges at the metal-binding site. The first approach was to create two variants to reduce charge repulsion in CD2.trigger by mutating the negatively charged residues. Mutant R31D/K43N replaced a negatively charged Asp with a neutral Asn at position 43. Mutant R31K/K43D replaced an Asp in CD2.trigger with a positively charged Lys at position 31 (Fig. 1). In contrast with the unfolded conformation of apo CD2.trigger, the R31K/K43D mutant exhibited the folded conformation at values up to pH 9 in the absence and presence of cations (Fig. 6D). The R31D/K43N mutant was also folded below pH 9 in the absence of cations (Fig. 6C, Fig. S3). In line with these experimental results, our electrostatic calculations predicted that the R31K/K43D and R31D/K43N mutations would increase the folding stability of CD2.trigger by 7.0 and 3.3 kcal·mol^{-1}, respectively. Although the magnitudes of the predictions from these crude calculations are questionable, they strongly suggest that modulations of charge–charge interactions constitute a dominant factor in the increase in folding stability by the R31K/K43D and R31D/K43N mutations. The experimental and calculated results for the R31K/K43D and R31D/K43N variants directly support the hypothesis that the unfolding of CD2.trigger in the apo form is a result of charge repulsion at the metal-binding site, and metal-induced folding is caused by a reduction in charge repulsion. Clearly, this 'hotspot' location of the Ca^{2+}-binding site is very sensitive to alterations in electrostatic interactions and charge repulsion (Fig. 1).

The thermal stability of CD2.trigger and its variants in the absence and presence of 10 mM Ca^{2+} was monitored using CD at 230 nm at pH 6.8. The three proteins showed similar far-UV CD spectra at low temperatures (5 °C), and underwent reversible thermal denaturation with the negative maximum shifting to 202 nm at high temperatures. The T_m values of the

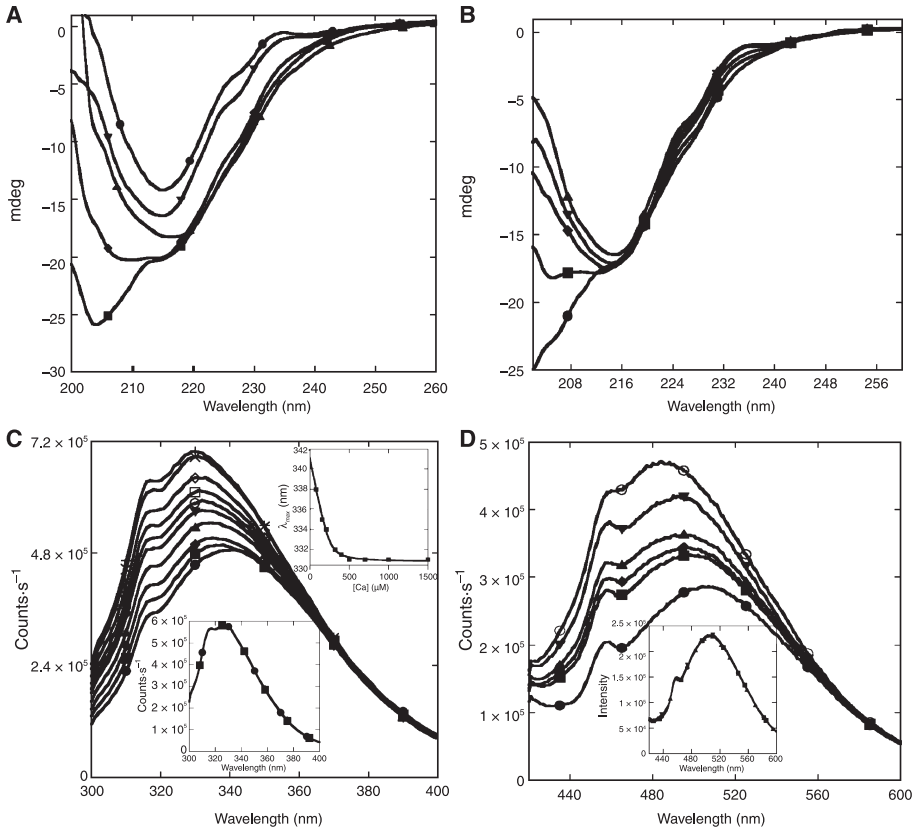

Fig. 3. Conformational studies as a function of metal ions. (A) Far-UV CD spectra of 10 μM wild-type CD2 (●) and 10 μM CD2.trigger in the presence of 1 mM EGTA (■), 10 mM Ca^{2+} (◆), 0.1 mM La^{3+} (▲) or 0.1 mM Tb^{3+} (▼) in 10 mM Tris at pH 7.2. (B) Far-UV CD spectral changes of CD2.trigger at varying Tb^{3+} concentrations in 20 mM Tris at pH 7.4. The Tb^{3+} concentrations were 0 (●), 1 (■), 2 (◆), 3 (▼) or 7 μM (▲). (C) Trp fluorescence of 2 μM CD2.trigger at Ca^{2+} concentrations of 0, 0.08, 0.16, 0.21, 0.32, 0.4, 0.5, 0.7, 1.0 or 1.5 mM (bottom to top) in 20 mM Tris at pH 8.0 (excited at 280 nm). The fitting of λ_{Max} of Trp emission as a function of Ca^{2+} concentration gave the K_d value of Ca^{2+} (inset top). The Trp fluorescence spectra of wild-type CD2 were overlaid at different Ca^{2+} concentrations (inset bottom). (D) Fluorescence emission spectra of 50 μM ANS only (●) and 50 μM ANS with the addition of 2 μM CD2.trigger in 20 mM Tris at pH 7.2 and in the presence of 0 (■), 1 (◆), 5 (▲), 7 (▼) or 10 μM (○) La^{3+} (excited at 394 nm). The λ_{Max} of emission was blue shifted and the fluorescence intensity was increased with increasing La^{3+} concentration, and the fluorescence intensity increased for wild-type CD2 (inset).

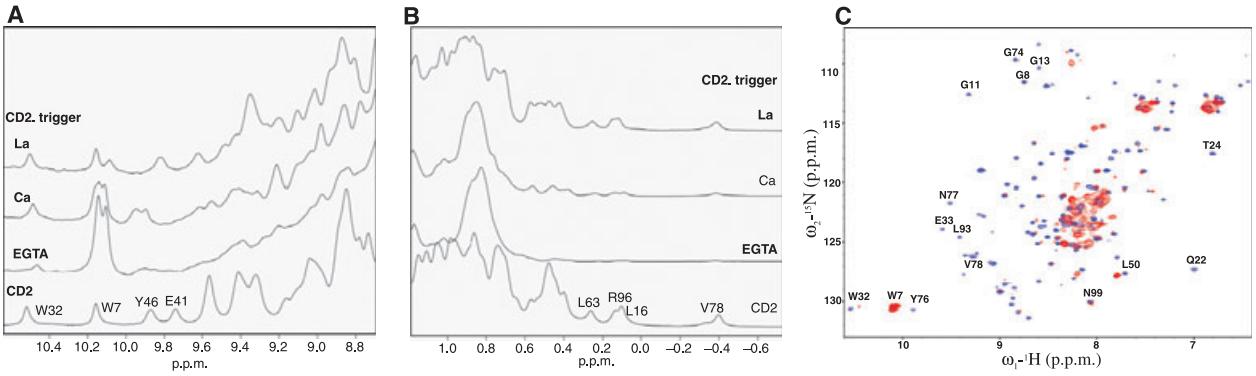

Fig. 4. NMR spectra. One-dimensional ^1H NMR spectra of CD2.trigger in the amide region (A) and the methyl group region (B) in the presence of 1 mM EGTA, 25 mM Ca^{2+} or 2 mM La^{3+}. The bottom spectrum is wild-type CD2 in 1 mM EGTA. Some of the assigned resonances of CD2 are labeled. (C) The major resonances of CD2.trigger in the heteronuclear single quantum correlation spectrum in the presence of 0.05 mM EGTA (red) are clustered in a narrow region, indicating the lack of well-packed tertiary structures. In the presence of 10 mM Ca^{2+} (blue), dispersed peaks, as in wild-type CD2, are observed, indicating the formation of a well-folded structure.

three proteins did not exhibit significant differences at pH 6.8 (Table 1).

The second approach was to lower the pH. Specifically, if the reduction in charge repulsion is the driving force for the metal-binding-induced conformational change, decreasing the pH should neutralize some of the negative coordination charges and thereby shift CD2.trigger towards the folded conformation. Consistent with this expectation, when the pH was decreased to below pH 7, CD2.trigger gradually converted to the native structure from its unfolded conformation (Fig. 5A), which closely resembled Ca^{2+}-, Tb^{3+}- or La^{3+}-induced refolding (Fig. 3A). The Trp fluorescence emission maximum was blue shifted to 327 nm at pH 7 (Fig. 6A). In addition, we observed a concurrent increase in the emission intensity, probably a result of the increased hydrophobicity of the Trp environment. The NMR (Fig. S2) spectra provided further evidence that the protonation-induced folding process was similar to the Ca^{2+}, Tb^{3+} or La^{3+}-induced folding process. The pH-dependent transition curves could be fitted with a two-state model. In the absence of metal ion, the transition pH values determined by the different spectroscopic methods were all close to pH 7.2 (Fig. 5B). The folding–unfolding transition pH was increased in the presence of Ca^{2+} or Tb^{3+}. Far-UV CD and Trp fluorescence studies showed that, at pH 7.4, CD2-trigger was predominantly unfolded in the absence of metal ion, but became predominantly folded in the presence of 7 μM Tb^{3+} (Fig. 3B) or 0.5 mM Ca^{2+} (Fig. 3C). In the presence of saturating amounts of cations, the apparent transition pH increased from 7.2 ± 0.1 to 8.5 ± 0.1 for Tb^{3+} (Fig. 5B). Folding or refolding was achieved by the addition of metal ions, a decrease in pH, or a combination of the two conditions. The effects of metal binding and protonation were additive.

Discussion

Electrostatic interactions and protein folding

The folding stability of proteins depends on delicate balances of noncovalent interactions, such as salt bridges, hydrogen-bonding networks, and van der Waals' and hydrophobic interactions. The electrostatic interactions between charged residues are long ranged. As a result of their strong favorable interactions with water, charged residues are predominantly located on the surface of proteins. Changes in salt concentrations or pH often have a significant effect on charge interactions.

Negatively charged residues are often observed around Ca^{2+}-binding pockets. Charged residues are important for tuning metal-binding affinity and selectivity [8,23]. However, in the absence of cation binding, the repulsion between charged residues often destabilizes the proteins. For example, Ca^{2+}-loaded CaM has high thermal stability with T_m > 90 °C, but the apo form is labile even at room temperature [32,33]. Furthermore, the removal of Ca^{2+} ions results in a molten globular state of α-lactalbumin [34]. Similarly, the introduction of a fifth charge in parvalbumin Ca^{2+}-binding sites results in a decrease in protein

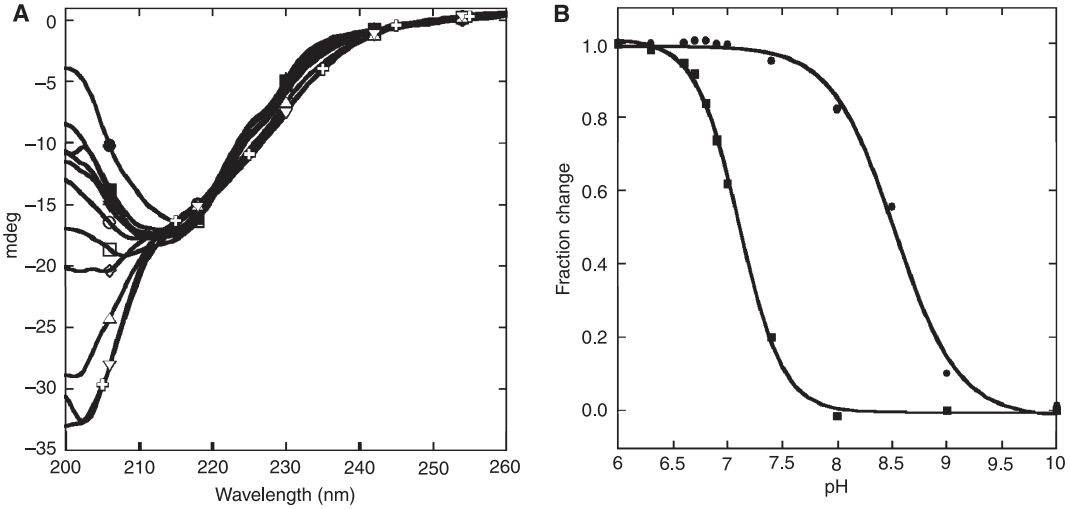

Fig. 5. Conformational studies as a function of pH. (A) Far-UV CD spectra of CD2.trigger at pH 9.0, 8.0, 7.4, 7.0, 6.8, 6.6, 6.4, 6.2, 6.0, 5.8 or 4.5 (bottom to top) in the absence of metal ion. (B) Signal changes of CD2.trigger as a function of pH in the absence (■) or presence (●) of 20 μM Tb^{3+}.

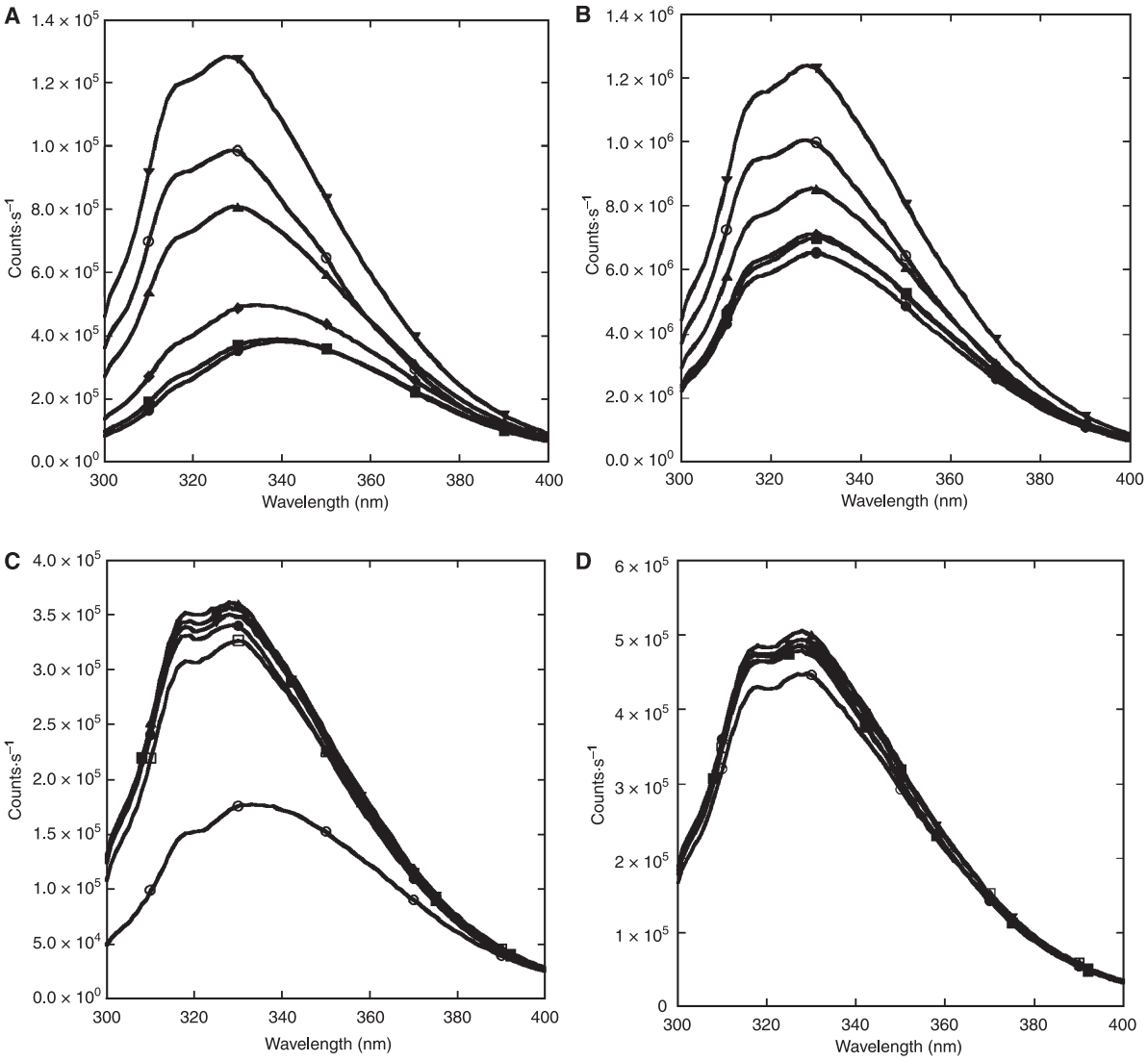

Fig. 6. Tryptophan emission fluorescence spectra. CD2.trigger spectra (excited at 280 nm) in the absence (A) or presence (B) of 0.5 mM Ca^{2+} at pH 9.0 (●), 8.5 (■), 8.0 (◆), 7.4 (▲), 7.0 (▼) or 6.5 (○), as well as R31D/K43N (C) and R31K/K43D (D) in acetate buffer (pH 4.0) in the presence of 1 mM EGTA (●) or 0.5 mM Ca^{2+} (■), in Pipes buffer (pH 6.8) in the presence of 1 mM EGTA (▲) or 0.5 mM Ca^{2+} (▼), and in Tris buffer (pH 9.0) in the presence of 1 mM EGTA (○) or 0.5 mM Ca^{2+} (□).

thermal stability in the absence of Ca^{2+} [35]. In addition to charge effects, Ca^{2+} binding may also result in changes in local conformations and dynamics that tune the function and stability of these proteins [36,37]. In natural proteins, Ca^{2+}-binding sites are almost all located within loop regions, turns or the ends of α-helices or β-sheets, probably as a result of their relatively higher flexibility [12].

To design Ca^{2+}-binding sites, we introduced charged and noncharged carboxyl residues in a non-Ca^{2+}-binding protein frame CD2. This mutation process results in proteins with different folding properties, depending on the nature of the changes, the number of charged residues and locations in the protein environment. Our first generation of designed Ca^{2+}-binding sites, such as that in CD2.Ca1, was created by mutating four core hydrophobic residues and one positively charged residue into four negatively charged residues [18–20]. This protein was largely unfolded in both apo and loaded forms. We then designed a second generation of Ca^{2+}-binding sites, such as Ca.CD2, which was capable of resisting global conformational changes on Ca^{2+} binding as a result of reducing either the number of mutations or the number of charged ligand residues. Interestingly, the Ca^{2+}-binding site in CD2.7E15, created by adding three negatively charged residues

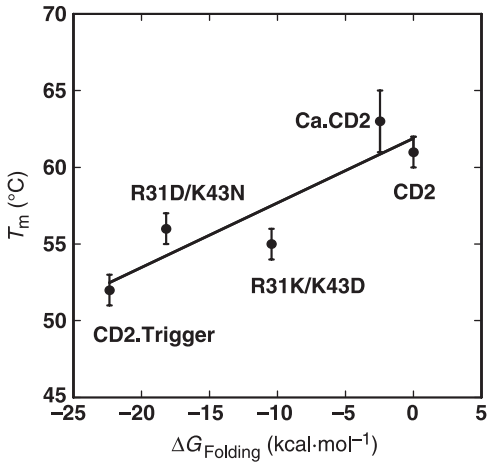

Fig. 7. Thermal transition temperature (T_m) of CD2 and its variants in the presence of 1 mM EGTA as a function of the calculated folding energy change ($\Delta G_{Folding}$) from wild-type CD2.

coupled with two existing residues Glu56 and Asp62, with a total of five negatively charged ligand residues, was able to retain native structure in the absence and presence of Ca^{2+}. It is also interesting to note that CD2.6D79, formed by the cluster of two new negative charges within β-strands, exhibited smaller backbone changes on mutation [22] compared with CD2.7E15 within loops [23], possibly as a result of the limited flexibility of the backbone and minimal perturbation of the native environment.

The alteration of electrostatic interactions may result in either an increase or decrease in protein stability [38,39]. In favorable cases, the effects on protein stability can be predicted by electrostatic calculations [40]. As shown in Fig. 7, the calculations predict that CD2.trigger and two mutants with altered charges at the Ca^{2+}-binding site have the following stability: wild-type CD2 > R31K/K43D > R31D/K43N > CD2.trigger. The cluster of negative charges designed into the Ca^{2+}-binding site of CD2.trigger presents an opportunity to validate these predictions. This predicted order is consistent with the measured melting temperatures of the five protein variants including Ca.CD2 at different locations. The electrostatic calculations thus provide corroborating evidence that the driving force for the metal-binding-induced folding of CD2.trigger is the decrease in charge repulsion present in the apo protein at pH 6.8. Furthermore, consistent with our observations, our electrostatic calculations predict that CD2.trigger has the lowest stability and Ca.CD2 has the highest stability in the absence of Ca^{2+} (Fig. 7).

Because a metal binds either preferentially or exclusively to the folded state, metal binding always increases the folding stability of a protein. The degree of increase depends on the binding affinity and the metal concentration. For example, Ca^{2+} shifts the T_m value of E-cadherin from 40 to 65 °C [41]. The T_m values of α- and β-parvalbumin CD-EF fragments increase by more than 20 °C as the Ca^{2+} concentration is moderately increased from 0.25 or 0.5 mM to 1 mM [39]. Conversely, the loss of Ca^{2+} binding often decreases the protein stability. We did not detect a change in T_m value for the R31K/K43D variant, but observed small increases in T_m for both CD2.trigger and the R31D/K43N variant. Given the fact that the different charged variants have almost identical CD spectra at high temperature, and the folding of the native conformation is Ca^{2+}, Tb^{3+} or La^{3+} specific, independent of excess Na^+ or K^+, it is less likely that the unfolded state is stabilized by the addition of extra surface negative charges.

Metal-induced conformational change in CD2.trigger

The design of CD2.trigger was based on our hypothesis that the clustering of charged coordination residues and the alteration of native electrostatic balance greatly destabilize the protein, and Ca^{2+} binding at the location will mitigate such effects. The single Ca^{2+}-binding site in CD2.trigger is located at a charge-sensitive 'hotspot' identified by electrostatic calculations. Using various spectroscopic methods, we have shown that the four proximate negative charges of Glu29, Asp31, Glu41 and Asp43 at the surface of the wild-type CD2 β-sandwich structure significantly destabilize the protein and result in the unfolding of the protein at room temperature at pH 7.4. At pH 6.8, the protein is folded as a result of neutralization of charge repulsion. Similarly, charge mutation by the R31D/K43N or R31K/K43D substitution stabilizes the folded state. The folding–unfolding process of CD2.trigger is reversible following a two-state model.

The pK_a value of wild-type CD2 has been examined using ^{15}N-labeled protein and site-directed mutagenesis [42]. Glu41 in wild-type CD2 has an unusually high pK_a value of 6.6, attributed to the hydrogen bond between protonated Glu41 and deprotonated Glu29 in close proximity. In principle, as nearby negative charges aid in protonation, the pK_a value of Glu41 in CD2.trigger is not likely to be lower than that in wild-type CD2. At high pH, it is reasonable to assume that the four proposed coordination residues in CD2.trigger possess four negative charges. On binding of Ca^{2+}, Tb^{3+} or La^{3+}, the net charges are reduced to −2 or −1. The effect of a pH change on the net charge of the

metal-binding site is dependent on the pK_a values of the residues. Therefore, a decrease to a slightly acidic pH 6.6 may significantly reduce the net negative charges at the metal-binding site. The folding of the protein under this condition allows us to conclude that the location of the CD2.trigger Ca^{2+}-binding site is capable of tolerating three negative charges. However, the repulsion introduced by the fourth charged residue exceeds the tolerance range of the β-strand of the wild-type CD2 Ig fold structure. The mutants R31K/K43D and R31D/K43N, with −2 and −3 charges in the binding site, respectively, maintain the wild-type CD2 structure in the absence of cations at basic pH, thus supporting the conclusions derived from the analysis of the pH study.

The observed enthalpy for Ca^{2+} binding to CD2.trigger is only -0.93 kcal·mol^{-1}. The small magnitude of ΔH may be caused by the protein undergoing an unfolded-to-folded transition on Ca^{2+} binding, attributable to a large change in conformational entropy. Such coupled folding–binding is reminiscent of natural trigger proteins with small heat releases. Several groups have reported that Ca^{2+} binding can lead to either heat release or absorbance depending on the site [31,39,43]. For example, the binding of Ca^{2+} to high-affinity sites in C2 domains is exothermic, whereas binding to low-affinity sites is endothermic [44]. Gilli *et al.* [29] have reported that Ca^{2+} binding to CaM has both an exothermic and an endothermic phase. Decreases in backbone entropy on Ca^{2+} binding have been determined by NMR relaxation for several proteins with high-affinity binding sites [37,45]. However, a study of one of our designed proteins has shown that the backbone entropy of the protein increases slightly on Ca^{2+} binding. For natural trigger proteins, because of the mutual influence of multiple metal-binding sites [21], the dissection of the relative contributions of specific interactions and conformational changes to Ca^{2+} binding is often controversial [29].

Design of trigger proteins

Extensive studies have been carried out to obtain an understanding of the molecular mechanisms of Ca^{2+}-dependent processes, with various approaches including the structural determination of apo and loaded forms of the trigger proteins. To date, the reported studies have focused mainly on natural Ca^{2+}-dependent proteins, such as CaM. The development of novel Ca^{2+}-dependent proteins has been attempted by mimicking natural Ca^{2+}-binding proteins which have multiple coupled metal-binding sites. Ababou & Desjarlais [13] abolished the Ca^{2+}-induced conformational change of N-terminal CaM by replacing its hydrophilic residues with large hydrophobic residues, as found in calbindin D_{9k}, which does not undergo global conformational change on Ca^{2+} binding. Conversely, Bunick *et al.* [14] built up the CaM-like Ca^{2+}-dependent conformational change in calbindin D_{9k} by replacing 15 residues in calbindin D_{9k} with the corresponding residues of CaM. Structural determination and other methods confirmed that the exposed hydrophobic surfaces on the Ca^{2+}-loaded form of the new protein were similar to those found on CaM.

Departing from previously reported methods, we did not rely on the use of sequence similarity between known Ca^{2+}-dependent proteins. The *de novo* design of CD2.trigger was achieved by coupling protein destabilization via the electrostatic repulsion between the introduced Ca^{2+} coordination residues and the re-acquisition of protein folding on Ca^{2+} binding. Previously, we have reported the success of designing several Ca^{2+}-binding proteins resistant to global conformational changes on Ca^{2+} binding [20,21,23]. The sites in these proteins were either partially located within flexible regions, or contained only two to three clustered negatively charged residues. Although the algorithms used to identify/design Ca^{2+}-binding sites were the same, we added major components to localize conformationally sensitive spots and to specifically incorporate electrostatic interactions that globally switch the conformation of the designed protein as a result of Ca^{2+}, Tb^{3+} or La^{3+} binding. To create Ca^{2+}-binding proteins with Ca^{2+}-induced global conformational change, we developed several new criteria to ensure a strong local charge interaction and strong metal binding, as well as methods to analyze and alter charge distribution on the host protein. In the absence of Ca^{2+}, CD2.trigger is highly dynamic and mobile, and possesses fewer tertiary structures than do natural trigger proteins, such as CaM or troponin C. To our knowledge, this is the first study to report the successful design of Ca^{2+}-, Tb^{3+}- or La^{3+}-induced trigger proteins with a single metal-binding site that do not rely on the use of sequence similarity to known Ca^{2+}-dependent proteins with multiple coupled metal-binding sites. The success in achieving a Ca^{2+}-dependent conformational change represents a major step forward from our previously published work.

Our design of a Ca^{2+}-binding trigger protein is significant for several reasons. First, this engineered protein can be utilized to study signal transduction systems involving Ca^{2+} [46], as well as Ca^{2+}-dependent cell adhesion [47], moving this achievement beyond design into functional application. Second,

the isolated metal-binding site in our design allows us to better elucidate key binding determinants, such as charge repulsions, that contribute to Ca^{2+} binding, and the resulting conformational changes. Data obtained from this strategy will provide insight into the mechanisms of Ca^{2+}-mediated signaling and the molecular bases for diseases associated with alterations in Ca^{2+} binding. Finally, these results provide guidance for the design of Ca^{2+}-switchable proteins, such as sensors or catalysts [48,49].

Materials and methods

Design of Ca^{2+}-binding site

The design of Ca^{2+}-binding sites was carried out on an SGI O2 computer using the METALFINDER program, as described previously [19,50]. The CD2 protein (Protein Data Bank code 1hng) was chosen as the scaffold. The protein surface potential was calculated using the DELPHI program on modeled structures. The modeled structure of the designed protein was generated by the design program, and the structures of its variants were generated using the SYBYL program (Tripos Co., St Louis, MO, USA).

Refinement of model structures by energy minimization

The structures of CD2.trigger and its R31K/K43D and R31D/K43N mutants were further refined using the AMBER program [51]. The Ca^{2+}-loaded structure of CD2.trigger generated by the SYBYL program was energy minimized within the AMBER ff99SB forcefield [52]. Minimization was completed in two stages. First, 2000 steps of minimization were carried out whilst the Ca^{2+}-loaded protein was restrained with a harmonic constant of 100 kcal·mol^{-1}·Å^{-1}. Second, 20 000 steps of minimization were carried out without restraints. Mutations were generated on the minimized CD2.trigger structure by the LEAP module in AMBER. The resulting mutated side-chain was energy minimized for at least 40 000 steps whilst the rest of the Ca^{2+}-loaded protein was fixed in space.

Effects of mutation on binding energy and folding stability

Electrostatic contributions of mutational effects on the Ca^{2+}-binding affinity and folding stability of CD2.trigger were calculated using the Poisson–Boltzmann (PB) equation. PB calculations were carried out using the UHBD program [53]. The calculation protocols on electrostatic contributions to protein binding and folding stability were followed, as described previously [40,54]. The protein and the solvent were modeled with dielectric constants of 4 and 78.5, respectively, with the dielectric boundary specified by the protein van der Waals' surface. The buffer was modeled as a 1 : 1 salt (with an ion exclusion radius of 2 Å) at a concentration of 20 mM and a temperature of 298 K. The solution of the PB equation started with a $150 \times 150 \times 150$ grid at a 1.5 Å spacing. This was followed by two levels of focusing, with the same grid dimensions but with the spacing reduced to 0.5 and 0.25 Å, respectively. The center of the second focusing grid was changed from the center of the protein to the site of mutation. The effect of a mutation on the Ca^{2+}-binding affinity was calculated as the change in the electrostatic binding free energy by the mutation. The electrostatic binding free energy was the difference in the total electrostatic free energy before and after Ca^{2+} binding:

$$\Delta G_b = G_{el}(Ca^{2+} - \text{protein}) - G_{el}(\text{protein}) - G_{el}(Ca^{2+}) \quad (1)$$

where the three terms on the right-hand side of Eqn (1) (from left to right) represent the electrostatic energies of the Ca^{2+}-loaded protein, the apo protein and the Ca^{2+} ion, respectively. In this calculation, the apo protein was assumed to have the same structure as the Ca^{2+}-loaded form. Similarly, the effect of a mutation on the folding stability was calculated as the change in the electrostatic folding free energy by the mutation. The electrostatic folding free energy was the difference in the total electrostatic free energy of the protein in the unfolded and folded states:

$$\Delta G_f = G_{el}(\text{protein}) - G_{el}(\text{residue}) \quad (2)$$

In this calculation, the folded protein was assumed to have the same structure as the Ca^{2+}-loaded form, even though the ion was absent. The unfolded state was modeled as the individual residues separately dissolved in the solvent. As the quantity of interest was the change in ΔG_f caused by the mutation, and the contributions of all separately dissolved residues other than that being mutated were identical before and after the mutation, only the electrostatic free energy of the residue being mutated, G_{el}(residue), was required to model the unfolded state.

Protein engineering and purification

The cloning, expression and purification of CD2.trigger followed established methods for glutathione *S*-transferase fusion proteins with minor modifications [19,20]. Briefly, the cell was lysed with 1% *N*-lauroylsarcosine sodium in pH 7.0 Tris buffer, with the addition of 5 mM dithiothreitol, 5 μM 4-(2-aminoethyl) benzenesulfonyl fluoride hydrochloride, 50 μM La^{3+} and 25 U·mL^{-1} Benzonase nuclease (Novagen, Madison, WI, USA). The glutathione *S*-transferase-fusion proteins were bound to a GS4-B affinity column (Amersham, Piscataway, NJ, USA) and cleaved on the column by thrombin (Amersham). The eluted protein

was further purified by Superdex G75 gel filtration chromatography (Amersham) and HiTrap SP cation exchange FPLC (Amersham). EGTA (0.5 mM) was added to the protein solution before HiTrap SP cation exchange FPLC to remove metal ions bound to the protein.

Fluorescence, CD and NMR spectra

All fluorescence, CD and NMR spectra were collected as described previously [19,20]. The dye ANS (Sigma Co., St Louis, MO, USA) in 20 mM Tris, pH 7.2, was titrated with La^{3+} in the presence and absence of proteins, and 10 min was allowed for equilibrium at each data point. The emission scans were acquired from 425 to 700 nm with excitation at 364 nm. For the CD study, the metal-free protein (10 μM) sample contained 1 mM EGTA, and the cation-loaded samples contained 10 mM Ca^{2+} or 0.1 mM La^{3+} or Tb^{3+}. The pH was varied from 5.8 to 9.0 for the pH study. For the thermal stability study, the temperature was increased from 5 to 90 °C at 2 °C increments, with a 10 min equilibration time at each temperature. Protein samples (10 μM) contained 1 mM EGTA or 10 mM Ca^{2+}. The metal-binding affinities were derived from metal titrations by fitting the signal changes from CD, fluorescence or NMR as a function of metal concentration, assuming the formation of a 1 : 1 protein–cation complex, as described previously [19,20].

ITC

The ITC experiment was performed using a VP-ITC instrument (MicroCal, LLC). The sample cell contained 0.1 mM of protein in 20 mM Pipes/10 mM KCl at pH 6.8. The injection solution contained 5 mM Ca^{2+} in the same buffer, and a volume of 2 μL was injected each time. The reference power was 5 $\mu cal \cdot s^{-1}$. The initial delay time was 300 s and the stirring speed was 280 r.p.m. The cell temperature was set to 5 °C. The sample cell and syringe were pretreated with 20 mM EGTA and washed with 20 mM Pipes/10 mM KCl at pH 6.8. All solutions for metal-binding studies were pretreated with Chelex-100 (Bio-Rad, Hercules, CA, USA). The data were analyzed using MICROCAL ORIGIN software (Microcal Software Co., Northampton, MA, USA).

Acknowledgements

We would like to thank Dan Adams, Michael Kirberger and Julian Johnson for critical review of the manuscript and helpful discussions, and David W. Wilson for assistance in running the ITC. This work was supported in part by the following sponsors: NIH GM070555, NIH GM62999 and NSF MCB-0092486 to JJY; NIH GM058187 to HXZ; and the Equipment Funds from the Georgia Research Alliance.

References

1 Ikura M & Ames JB (2006) Genetic polymorphism and protein conformational plasticity in the calmodulin superfamily: two ways to promote multifunctionality. *Proc Natl Acad Sci USA* **103**, 1159–1164.
2 Kretsinger RH (1976) Calcium-binding proteins. *Annu Rev Biochem* **45**, 239–266.
3 Klee CB, Crouch TH & Richman PG (1980) Calmodulin. *Annu Rev Biochem* **49**, 489–515.
4 Meador WE, Means AR & Quiocho FA (1993) Modulation of calmodulin plasticity in molecular recognition on the basis of x-ray structures. *Science* **262**, 1718–1721.
5 Chou JJ, Li S, Klee CB & Bax A (2001) Solution structure of Ca(2+)-calmodulin reveals flexible hand-like properties of its domains. *Nat Struct Biol* **8**, 990–997.
6 Frederick KK, Marlow MS, Valentine KG & Wand AJ (2007) Conformational entropy in molecular recognition by proteins. *Nature* **448**, 325–329.
7 Reid RE & Hodges RS (1980) Co-operativity and calcium/magnesium binding to troponin C and muscle calcium binding to parvalbumin: an hypothesis. *J Theor Biol* **84**, 401–444.
8 Falke JJ, Drake SK, Hazard AL & Peersen OB (1994) Molecular tuning of ion binding to calcium signaling proteins. *Q Rev Biophys* **27**, 219–290.
9 Linse S & Forsen S (1995) Determinants that govern high-affinity calcium binding. *Adv Second Messenger Phosphoprotein Res* **30**, 89–151.
10 Glusker JP (1991) Structural aspects of metal liganding to functional groups in proteins. *Adv Protein Chem* **42**, 1–76.
11 Zhou Y, Yang W, Kirberger M, Lee HW, Ayalasomayajula G & Yang JJ (2006) Prediction of EF-hand calcium-binding proteins and analysis of bacterial EF-hand proteins. *Proteins* **65**, 643–655.
12 Pidcock E & Moore GR (2001) Structural characteristics of protein binding sites for calcium and lanthanide ions. *J Biol Inorg Chem* **6**, 479–489.
13 Ababou A & Desjarlais JR (2001) Solvation energetics and conformational change in EF-hand proteins. *Protein Sci* **10**, 301–312.
14 Bunick CG, Nelson MR, Mangahas S, Hunter MJ, Sheehan JH, Mizoue LS, Bunick GJ & Chazin WJ (2004) Designing sequence to control protein function in an EF-hand protein. *J Am Chem Soc* **126**, 5990–5998.
15 Batey S, Randles LG, Steward A & Clarke J (2005) Cooperative folding in a multi-domain protein. *J Mol Biol* **349**, 1045–1059.
16 Yang JJ, Gawthrop A & Ye Y (2003) Obtaining site-specific calcium-binding affinities of calmodulin. *Protein Pept Lett* **10**, 331–345.

17 Ye Y, Lee HW, Yang W, Shealy S & Yang JJ (2005) Probing site-specific calmodulin calcium and lanthanide affinity by grafting. *J Am Chem Soc* **127**, 3743–3750.
18 Yang W, Lee HW, Hellinga H & Yang JJ (2002) Structural analysis, identification, and design of calcium-binding sites in proteins. *Proteins* **47**, 344–356.
19 Yang W, Jones LM, Isley L, Ye Y, Lee HW, Wilkins A, Liu ZR, Hellinga HW, Malchow R, Ghazi M *et al.* (2003) Rational design of a calcium-binding protein. *J Am Chem Soc* **125**, 6165–6171.
20 Yang W, Wilkins AL, Ye Y, Liu ZR, Li SY, Urbauer JL, Hellinga HW, Kearney A, van der Merwe PA & Yang JJ (2005) Design of a calcium-binding protein with desired structure in a cell adhesion molecule. *J Am Chem Soc* **127**, 2085–2093.
21 Yang W, Wilkins AL, Li S, Ye Y & Yang JJ (2005) The effects of Ca^{2+} binding on the dynamic properties of a designed Ca^{2+}-binding protein. *Biochemistry* **44**, 8267–8273.
22 Jones LM, Yang W, Maniccia AW, Harrison A, van der Merwe PA & Yang JJ (2008) Rational design of a novel calcium-binding site adjacent to the ligand-binding site on CD2 increases its CD48 affinity. *Protein Sci* **17**, 439–449.
23 Maniccia AW, Yang W, Li SY, Johnson JA & Yang JJ (2006) Using protein design to dissect the effect of charged residues on metal binding and protein stability. *Biochemistry* **45**, 5848–5856.
24 Driscoll PC, Cyster JG, Campbell ID & Williams AF (1991) Structure of domain 1 of rat T lymphocyte CD2 antigen. *Nature* **353**, 762–765.
25 Jones EY, Davis SJ, Williams AF, Harlos K & Stuart DI (1992) Crystal structure at 2.8 Å resolution of a soluble form of the cell adhesion molecule CD2. *Nature* **360**, 232–239.
26 Wagner G (1995) E-cadherin: a distant member of the immunoglobulin superfamily. *Science* **267**, 342.
27 Yang JJ, Ye Y, Carroll A, Yang W & Lee HW (2001) Structural biology of the cell adhesion protein CD2: alternatively folded states and structure–function relation. *Curr Protein Pept Sci* **2**, 1–17.
28 Honig B & Nicholls A (1995) Classical electrostatics in biology and chemistry. *Science* **268**, 1144–1149.
29 Gilli R, Lafitte D, Lopez C, Kilhoffer M, Makarov A, Briand C & Haiech J (1998) Thermodynamic analysis of calcium and magnesium binding to calmodulin. *Biochemistry* **37**, 5450–5456.
30 Reddi AR & Gibney BR (2007) Role of protons in the thermodynamic contribution of a Zn(II)–Cys4 site toward metalloprotein stability. *Biochemistry* **46**, 3745–3758.
31 Griko YV & Remeta DP (1999) Energetics of solvent and ligand-induced conformational changes in alpha-lactalbumin. *Protein Sci* **8**, 554–561.
32 Protasevich I, Ranjbar B, Lobachov V, Makarov A, Gilli R, Briand C, Lafitte D & Haiech J (1997) Conformation and thermal denaturation of apocalmodulin: role of electrostatic mutations. *Biochemistry* **36**, 2017–2024.
33 Tsalkova TN & Privalov PL (1985) Thermodynamic study of domain organization in troponin C and calmodulin. *J Mol Biol* **181**, 533–544.
34 Schulman BA, Kim PS, Dobson CM & Redfield C (1997) A residue-specific NMR view of the non-cooperative unfolding of a molten globule. *Nat Struct Biol* **4**, 630–634.
35 Henzl MT, Hapak RC & Goodpasture EA (1996) Introduction of a fifth carboxylate ligand heightens the affinity of the oncomodulin CD and EF sites for Ca^{2+}. *Biochemistry* **35**, 5856–5869.
36 Smallridge RS, Whiteman P, Werner JM, Campbell ID, Handford PA & Downing AK (2003) Solution structure and dynamics of a calcium binding epidermal growth factor-like domain pair from the neonatal region of human fibrillin-1. *J Biol Chem* **278**, 12199–121206.
37 Gagne SM, Tsuda S, Spyracopoulos L, Kay LE & Sykes BD (1998) Backbone and methyl dynamics of the regulatory domain of troponin C: anisotropic rotational diffusion and contribution of conformational entropy to calcium affinity. *J Mol Biol* **278**, 667–686.
38 Strickler SS, Gribenko AV, Gribenko AV, Keiffer TR, Tomlinson J, Reihle T, Loladze VV & Makhatadze GI (2006) Protein stability and surface electrostatics: a charged relationship. *Biochemistry* **45**, 2761–2766.
39 Henzl MT, Agah S & Larson JD (2003) Characterization of the metal ion-binding domains from rat alpha- and beta-parvalbumins. *Biochemistry* **42**, 3594–3607.
40 Dong F & Zhou HX (2002) Electrostatic contributions to T4 lysozyme stability: solvent-exposed charges versus semi-buried salt bridges. *Biophys J* **83**, 1341–1347.
41 Prasad A & Pedigo S (2005) Calcium-dependent stability studies of domains 1 and 2 of epithelial cadherin. *Biochemistry* **44**, 13692–13701.
42 Chen HA, Pfuhl M, McAlister MS & Driscoll PC (2000) Determination of pK(a) values of carboxyl groups in the N-terminal domain of rat CD2: anomalous pK(a) of a glutamate on the ligand-binding surface. *Biochemistry* **39**, 6814–6824.
43 Jelesarov I & Bosshard HR (1999) Isothermal titration calorimetry and differential scanning calorimetry as complementary tools to investigate the energetics of biomolecular recognition. *J Mol Recognit* **12**, 3–18.
44 Torrecillas A, Laynez J, Menendez M, Corbalan-Garcia S & Gomez-Fernandez JC (2004) Calorimetric study of the interaction of the C2 domains of classical protein kinase C isoenzymes with Ca^{2+} and phospholipids. *Biochemistry* **43**, 11727–11739.
45 Akke M, Skelton NJ, Kordel J, Palmer AG III & Chazin WJ (1993) Effects of ion binding on the backbone

dynamics of calbindin D9k determined by ^{15}N NMR relaxation. *Biochemistry* **32**, 9832–9844.
46 Hofer AM & Brown EM (2003) Extracellular calcium sensing and signalling. *Nat Rev Mol Cell Biol* **4**, 530–538.
47 Kemler R, Ozawa M & Ringwald M (1989) Calcium-dependent cell adhesion molecules. *Curr Opin Cell Biol* **1**, 892–897.
48 Mizoue LS & Chazin WJ (2002) Engineering and design of ligand-induced conformational change in proteins. *Curr Opin Struct Biol* **12**, 459–463.
49 Lu Y, Berry SM & Pfister TD (2001) Engineering novel metalloproteins: design of metal-binding sites into native protein scaffolds. *Chem Rev* **101**, 3047–3080.
50 Deng H, Chen G, Yang W & Yang JJ (2006) Predicting calcium-binding sites in proteins – a graph theory and geometry approach. *Proteins* **64**, 34–42.
51 Case DA, Darden TA, Cheatham TE III, Simmerling CL, Wang J, Duke RE, Luo R, Merz KM, Pearlman DA, Crowley M *et al*. (2006) AMBER 9. University of California, San Francisco, CA.
52 Hornak V, Abel R, Okur A, Strockbine B, Roitberg A & Simmerling C (2006) Comparison of multiple Amber force fields and development of improved protein backbone parameters. *Proteins* **65**, 712–725.
53 Madura JD, Briggs JM, Wade R, Davis ME, Luty BA, Ilin A, Antosiewicz J, Gilson MK, Bagheri B, Scott LR *et al*. (1995) Electrostatics and diffusion of molecules in solution: simulations with the University of Houston Brownian Dynamics program. *Comput Phys Commun* **91**, 57–95.
54 Dong F, Vijayakumar M & Zhou HX (2003) Comparison of calculation and experiment implicates significant electrostatic contributions to the binding stability of barnase and barstar. *Biophys J* **85**, 49–60.

Supporting information

The following supplementary material is available:
Fig. S1. Mass spectrum of CD2.trigger in the presence of a 20-fold molar excess of $LaCl_3$.
Fig. S2. NMR spectra. One-dimensional NMR spectra of CD2.trigger in the absence of divalent and trivalent cations at pH 7.4, 7.2, 7.0, 6.6 and 6.1 (bottom to top).
Fig. S3. Far-UV CD spectra of R31D/K43N (A) and R31K/K43D (B) at pH values ranging from 7.3 to 5.4.
Fig. S4. Metal-binding affinity.

This supplementary material can be found in the online version of this article.

Please note: Wiley-Blackwell are not responsible for the content or functionality of any supplementary material supplied by the authors. Any queries (other than missing material) should be directed to the corresponding author for the article.